Springer

KSME

Journal of Mechanical Science and Technology 24 (8) (2010) 1717~1728
www.springerlink.com/content/1738-494x
DOI 10.1007/s12206-010-0504-3

Predictive position and force control for shape memory alloy cylinders †

Nguyen Trong Tai[1], Nguyen Bao Kha[1] and Kyoung Kwan Ahn[2,*]

[1]*Graduate School of Mechanical and Automotive Engineering, University of Ulsan, Korea*
[2]*School of Mechanical and Automotive Engineering, University of Ulsan, Korea*

(Manuscript Received May 15, 2009; Revised April 7, 2010; Accepted April 11, 2010)

Abstract

In this paper, a linear lightweight electric cylinder constructed using shape memory alloy (SMA) is proposed. Spring SMA is used as the actuator to control the position and force of the cylinder rod. The model predictive control algorithm is investigated to compensate SMA hysteresis phenomenon and control the cylinder. In the predictive algorithm, the future output of the cylinder is computed based on the cylinder model, and the control signal is computed to minimize the error and power criterion. The cylinder model parameters are estimated by an online identification algorithm. Experimental results show that the SMA cylinder is able to precisely control position and force by using the predictive control strategy though the hysteresis effect existing in the actuator. The performance of the proposed controller is compared with that of a conventional PID controller.

Keywords: SMA cylinder; Force; Position; Predictive control; Real time; Online estimation; Online identification

1. Introduction

Shape memory alloy (SMA) actuators, which can return to their original shape at a preset temperature, possess interesting properties in terms of force generation capacity, potential for miniaturization, and power consumption. The forces exerted by the contraction of SMA actuators, along with their small diameters, light weights, and simplicity of operation make SMA actuators worthy of consideration as electrically controlled actuators, for use in applications such as robot grippers [1] or micropump [2].

In this work, an electric cylinder using an SMA spring was fabricated. The position and force generated from the operation of this cylinder are also investigated.

Although the nonlinearity hysteresis effect that exists in SMA actuators has significant potential applications in control systems, it also introduces delays and leads to inaccuracy in the control of these actuators. This phenomenon is also encountered in many applications that involve SMA, magnetic materials, or piezoelectric actuators. In order to achieve good performance of the control system, hysteresis phenomenon must be compensated. Many studies have investigated control methods to compensate for SMA hysteresis phenomenon. In [3], the SMA actuator is modeled and a gain schedule controller is applied to the control. In [4], the SMC method is used to control the SMA. In [5-6], a PID tuning controller and IMC were applied to control the SMA. These controllers yielded good tracking control results, but there was chattering in the input control signal. Most of these works required a precise system model, which makes the controller synthesis complicated and time consuming. In [7], the neural network is used to identify the inverse model of the SMA, and the model is then used to control the SMA. To compensate the model error, the feed-forward controller, PID controller, and sliding mode controller were added to the controller, thus making the controller bulky, complicated, and time-consuming for inverse model identification.

Generalized predictive control (GPC) is one of the most powerful and useful model-based control methods for a wide class of nonlinear dynamic systems [8-12]. The basic principle of GPC is to generate a sequence of control signals at each sample interval that optimizes the control effort, in order to follow the reference trajectory exactly.

In this study, GPC is proposed as a method to compensate the SMA hysteresis phenomenon. The GPC strategy is optimized to the control error and power consumption, thus it reduces the control error and chattering. Besides, with the model identified online, the nonlinear characteristic is identified, so the hysteresis phenomenon is compensated. The GPC control scheme is used to generate a control sequence by minimizing a cost function in such a way that the future force output is driven close to reference over a finite prediction horizon. The objective of this paper is to investigate this control

† This paper was recommended for publication in revised form by Associate Editor Hyoun Jin Kim

*Corresponding author. Tel.: +82 52 259 2282, Fax.: +82 52 259 1680
E-mail address: kkahn@ulsan.ac.kr

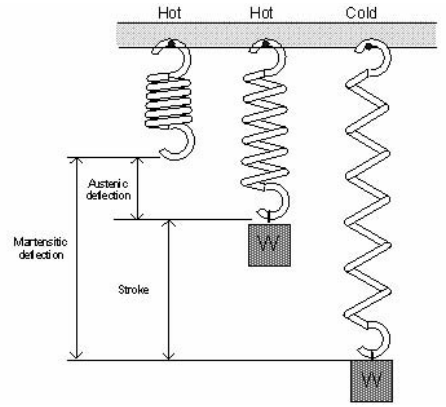

Fig. 1. Extension spring deflections.

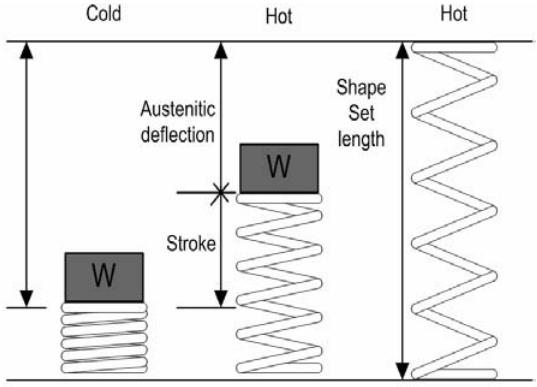

Fig. 2. Compression spring deflections.

strategy for improving the control performance of slow response SMA actuators.

The remainder of the paper is organized as follows. Section 2 describes the fabrication and experimental setup of the proposed SMA cylinder. Section 3 presents the algorithm applied to the position and force control of the SMA actuator. This includes a brief review of the online identification method using recursive parameter estimation and the implementation of the predictive algorithm in real time control. Section 4 compares experimental results for position and force control of the SMA actuator obtained from the predictive control algorithm with those from conventional PID control. Section 5 provides concluding remarks.

2. Fabrication and experimental setup of the SMA cylinder

The first part of this section presents the design principle of actuators using SMA springs. The fabrication of a SMA cylinder and the experimental setup are described in the second part of this section.

2.1 Actuator design using SMA springs

With the possible exception of straight wire, the most popular and useful form of SMA material is as SMA springs. Such springs can be used either in extension (tension) or compression, can provide an impressively large stroke, and can be designed to exert significant forces. Both extension and compression springs can be made from SMA materials. As illustrated in Fig. 1, an extension provides a pulling force by contracting when transformed to the high temperature austenitic state. The close coiled, zero load configuration of the extension spring is the shape that is *remembered* at high temperature.

A compression spring provides a pushing force by extending at high temperature, as shown in Fig. 2. The length to which a compression spring is shape-set is similar to the free length of a steel spring, and all deflections are determined with respect to that length.

2.1.1 Spring SMA parameter design

The design procedure can be divided into two stages: determination of the wire diameter by constraining the maximum shear stress and the spring index, and determination of the number of active turns in the spring through constraint of the shear strain. These parameters are computed using the design equations in [13] as follows:

▪ *Determination of wire diameter:*

Wire diameter of a spring SMA is determined as:

$$d = \sqrt{8W.P.c/\pi\tau_c}\ [mm] \tag{1}$$

Where P is the total force required from the SMA spring at high temperature: $P = F_n + F_h$.

F_n : required net output force.

F_h : force exerted by the bias spring.

τ_c is the maximum shear stress of the SMA spring.

c is the spring index, which depends on the average diameter D and wire diameter d of the spring:

$c = D/d$

W is the Wahl correction factor, which depends on the spring index c, $W = \frac{4c-1}{4c-4} + \frac{0.615}{c}$

▪ *Determination of number of turns:*

The number of turns in the spring can be obtained from:

$$n = \frac{d.S}{\pi D^2.\Delta\gamma} \tag{2}$$

where S is the stroke of the actuator, $\Delta\gamma$ is the strain difference at high and low temperature: $\Delta\gamma = \gamma_L - \gamma_H$

The shear strains are computed from shear stress and shear modulus as follows:

$\gamma_H = \tau_H / G_H$, $\gamma_L = \tau_L / G_L$

$\tau_H = \tau_c$, τ_L are shear strains at high and low temperatures, respectively.

G_H, G_L are shear modulus at high and low temperatures, respectively.

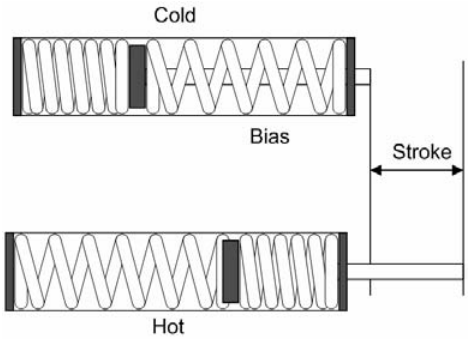

Fig. 3. Shape memory spring with biasing spring.

- *High temperature spring rate:*

$$K_h = 2588B[N/mm] \quad (3)$$

where $B = d/nc^3$

- *Low temperature spring rate:*

$$K_l = 345B \quad [N/mm] \quad (4)$$

- *Low temperature length:*

$$L_l = d(n+3) \quad [mm] \quad (5)$$

- *High temperature length:*

$$L_h = L_l + S \quad [mm] \quad (6)$$

- *Free length:*

$$L_f = L_h + P/K_h \quad [mm] \quad (7)$$

- *Reset force:*

$$F_r = K_l(S + P/K_h) \quad [N] \quad (8)$$

2.1.2 Design using bias springs

The system using a SMA spring and a bias spring is self resetting. That is, the constant load applied by the weight deforms the shape memory spring at the lower temperature. In most practical situations, a conventional steel spring provides a bias force to reset the shape memory spring at low temperatures, as shown in Fig. 3.

The shape memory spring has to work against an ever-increasing force from the biasing spring, and the net force output of the spring diminishes as the temperature increases. The desired parameter for a steel spring can be derived as follows:

- *Bias rare:*

$$K_b = \frac{F_h - F_l}{S} \quad [N/mm] \quad (9)$$

- *Bias wire diameter:*

$$d_b = \sqrt[3]{\frac{2.55F_hD_b}{T}} \quad [mm] \quad (10)$$

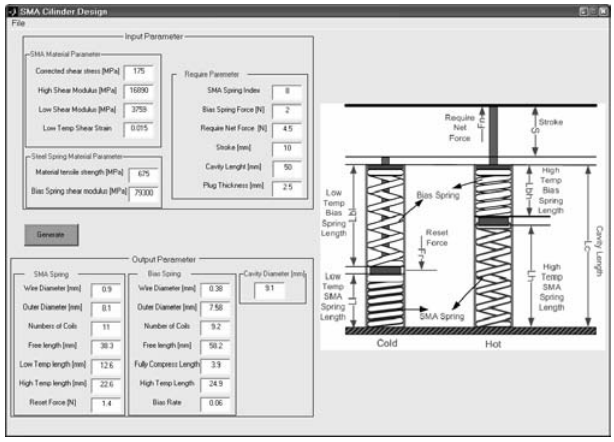

Fig. 4. SMA Cylinder design tool and design results.

where:

D_b is the average bias spring diameter.

T is the maximum bias shear stress.

- *Number of bias active turns:*

$$n = \frac{Gd_b^4}{8D_b^3K_b} \quad (11)$$

where G is the steel spring modulus.

- *Bias spring length at high temperature:*

$$L_{bh} = cavity\,length - plug\,thickness - L_h \quad [mm] \quad (12)$$

- *High temperature bias deflection:*

$$\delta = F_h/K_b \quad [mm] \quad (13)$$

- *Number of bias active turns:*

$$L_{bf} = L_{bh} + \delta \quad [mm] \quad (14)$$

2.1.3 Design using cylinder

A cylinder is designed and fabricated to satisfy the following parameters:

- Maximum Force: 4 N.
- Stroke: 10 mm.
- Life time: 50,000 cycles.
- Cavity: Length 50 mm.

Using equations Eq. (1) to Eq. (14), a Matlab tool is designed to compute the parameters of the SMA spring and steel spring for the required cylinder. That tool is shown in Fig. 4.

A Ni-Ti SMA spring is used with the following material parameters:

- Maximum shear stress: $T_C = 175\ MPa$.
- Transformation temperatures: $A_f = 56^0C$ (heating), $M_f = 33^0C$ (cooling).
- Shear modulus: $G_H = 16890\ MPa$ (high temperature), $G_L = 3759\ MPa$ (low temperature).
- Choose:
  - Spring index: $c = 8$.

- Low temperature shear strain: $\gamma_l = 0.015$ (in order to satisfy the life time requirement of 50,000 cycles).

With a standard steel spring, we have:

- Maximum shear stress: $T = 675\ MPa$.
- Shear modulus: $G_h = 79300\ MPa$.
- Assume that the force exerted by the steel spring is $F_h = 2N$

The required parameters of SMA and steel spring are shown in Fig. 4.

2.2 Experimental setup

The experimental actuator configuration and a photograph of the actuator are shown in Figs. 5 and 6, respectively. A 15.5 turns standard SMA spring with 8 mm outer diameter and 0.95 mm wire made by the Memory – Metalle GmbH Company is used to provide 4.042 N force and 15.082 mm. This standard SMA is close to the designed SMA, and satisfies the requirements in section 2.1. A steel spring used to provide a bias force to reset the shape memory spring at low temperature is fixed to the platform at one end. The other end of the bias spring is connected to the cylinder rod by an insulated wire. The SMA spring has an electrical connection at each end through electrical lugs crimped over a knot tied in the wire. The lugs also allow the spring ends to be secured to a terminal block. This terminal block is mobile, and can be positioned by means of a screw. The SMA spring is insulated from the cylinder rod by some plastic rings.

As soon as the SMA spring is heated by a current, the force exerted by that spring increases, and causes the cylinder rod to move in one direction. The bias spring creates the force to reset the shape memory spring at a lower temperature, and therefore causes the cylinder rod to move in the oposite direction.

Fig. 7 shows the experimental setup for measurment and control of the proposed SMA actuator. Position and force control of the SMA cylinder are both investigted in this system. Displacement of the cylinder rod is measured by a high precision potentiometer (Copal Electronics). The force exerted by the SMA cylinder is measured by a FlexiForce sensor (Tekscan) as shown in Fig. 8. These feedback signals are fed to the computer through an A/D Advantech PCI-1711 card. The control current applied to the SMA wire is obtained from a D/A card and a V/I converter. This system is controlled in real-time with the Real-time Windows Target Toolbox of Matlab.

3. Predictive control for position and force of SMA actuators

This section presents the predictive control algorithm used to control the position and force of the proposed SMA cylinder. Since the predictive control strategy generates the control signal based on the predicted output behaviour of the SMA systems, it can be applied to improve the control performance of SMA actuators.

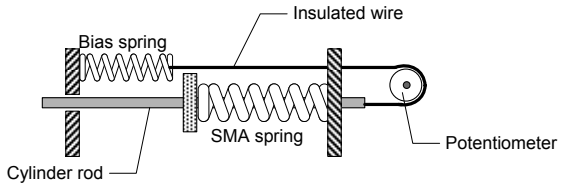

Fig. 5. Experimental SMA actuator configuration.

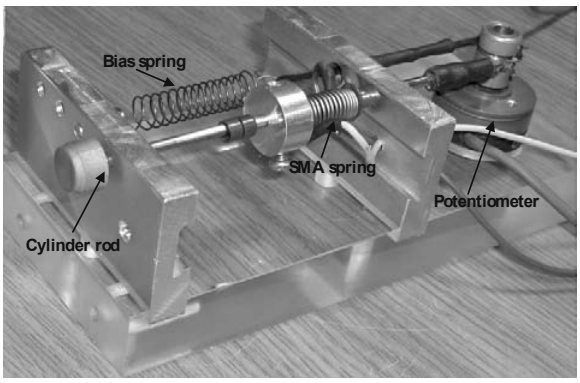

Fig. 6. Photo of Experimental SMA actuator.

3.1 Principal ideas of predictive control

Predictive control uses a model of the plant to predict the future output of the system. Based on this prediction, at each sampling period, a sequence of future control values is elaborated through an on-line optimization process, which minimizes the cost function of error and energy. Only the first value of this optimal sequence is applied to the plant; the whole procedure is repeated at the next sampling period according to the *receding* horizon strategy [14-15].

The following cost function is constructed in such a way that the future output $y(t)$ is driven close to the reference $r(t)$:

$$J(u,t) = E\left\{\sum_{j=N_1}^{N_2}\left[y(t+j) - r(t+j)\right]^2 + \lambda\sum_{j=1}^{N_u}\left[\Delta u(t+j-1)\right]^2\right\} \tag{15}$$

where $y(t+j)$ is the j -step prediction of the system output based on the data up to time *t, r(t+j)* is the future reference signal, λ is a weight coefficient to penalize the control sequence, and $E\{.\}$ is the expectation operator, which indicates the computation of control values for data up to time t and the stochastic disturbance model. N_1, N_2 and N_u are the minimum prediction horizon, maximum prediction horizon, and control horizon, respectively.

This cost function evaluates the error between the predicted output y and reference r in a prediction range from $t+N_1$ to $t+N_2$. The function also evaluates the control signal in a control range from t to $t+N_u$.

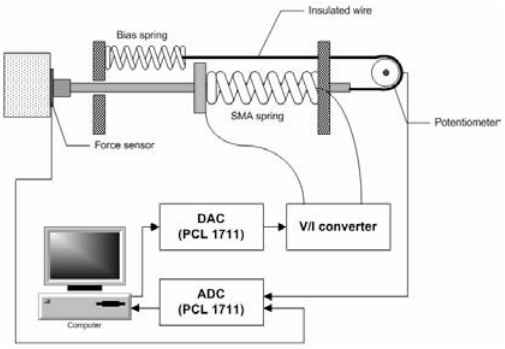

Fig. 7. Experimental setup for SMA cylinder.

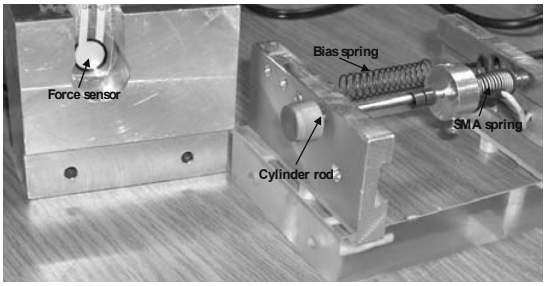

Fig. 8. SMA cylinder and force sensor.

The predictive control and its working principle are shown in Fig. 9.

In this study, the model of the plant is estimated by the online identification method, which is presented in Section 3.2. The solution of the output control is presented in Sections 3.3 and 3.4.

3.2 Online system identification

In order to predict the future output for the position and exerted force of the SMA actuators, it is necessary to obtain the dynamic model through the on-line system identification. In this section, the non-linear model of the SMA cylinder can be identified by using an approximately linearized method.

The idea of identification is presented in Ljung 1999 [16]. Around operating point, the input-output relationship can be described by the following linear difference equation as:

$$\begin{aligned} &y(k)+a_1y(k-1)+...a_{na}y(k-na) \\ &\quad = b_1u(k-1-d)+...b_{nb}(k-nb-d)+\varepsilon(k) \end{aligned} \tag{16}$$

where:

$y(k)$ is the output at sample time k;

$u(k)$ is control signal sample time k;

$\varepsilon(k)$ is model error and/or white noise;

d is time delay;

na, nb are the order of the denominator and numerator, respectively.

Define:

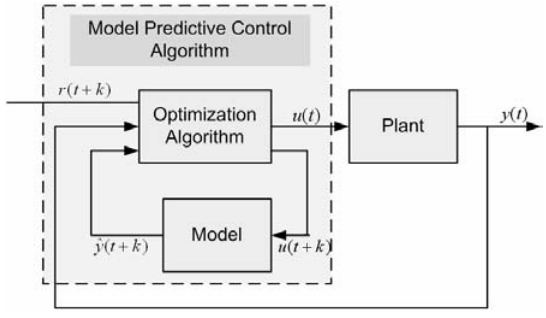

(a)

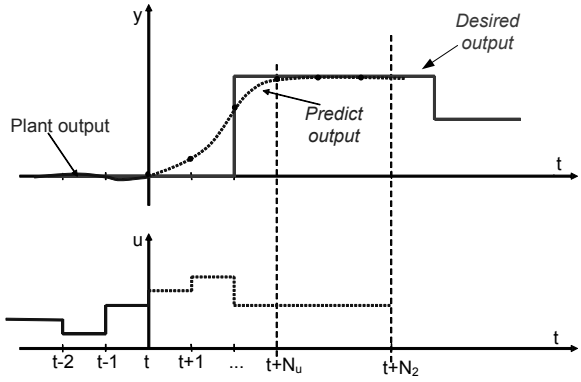

(b)

Fig. 9. General Predictive Control Diagram and Predictive Principle.

$$\theta = \left[a_1\ a_2\ ...a_{na}\ b_1\ b_2\ ...\ b_{nb}\right]^T = \left[\theta_1\ \theta_2\ ...\theta_{na+nb}\right]^T \tag{17a}$$

$$\begin{aligned} \varphi(k) = \big[&-y(k-1)-y(k-2)\ ...-y(k-na)... \\ &u(k-1-d)\ u(k-2-d)\ ...u(k-nb-d)\big]^T \end{aligned} \tag{17b}$$

and Eq. (16) can be written in the form:

$$y(k\,|\,\theta) = \varphi^T(k)\theta + \varepsilon(k) \tag{18}$$

The objective of the off-line identification problem is to find the parameter vector θ in Eq. (17a), such that the error $\varepsilon(t)$ is minimized. The formal objective function is a quadratic criterion.

$$J(\theta,t) = \frac{1}{2}\sum_{i=1}^{N}\left[y(i)-\varphi^T(i)\theta\right]^2 = \frac{1}{2}\sum_{i=1}^{N}\left(\varepsilon(i)\right)^2 \tag{19}$$

where N is the size of the known experimental data of the system.

However, in most control systems, when the system is identified on-line, the parameters θ_i may not be constant. They can be varied instantaneously. The parameters may change suddenly or slowly in this case. The criterion Eq. (15) is modified according to the following:

$$J(\theta,t) = \frac{1}{2}\sum_{i=1}^{k}\lambda^{k-i}(y(i)-\varphi^T(i)\theta)^2 \tag{20}$$

This criterion has been used to measure how well the model fits the experimental data from $t=1$ to N.

In this criterion, the parameter $\lambda(0<\lambda\leq 1)$ is called the forgetting factor: The most recent data point is $\lambda=1$, but data points that are n time units old are weighted by λ^n.

The results of parameter estimation to minimize Eq. (20) are obtained by using the recursive least-squares algorithm [16] as follows:

$$\hat{\theta}(k)=\hat{\theta}(k-1)+K(k)\left[y(k)-\varphi^T(k)\hat{\theta}(k-1)\right] \tag{21a}$$

$$K(t)=P(k)\varphi(k)=\frac{P(k-1)\varphi(k)}{\lambda(k)+\varphi^T(k)P(k-1)\varphi(k)} \tag{21b}$$

$$P(k)=\frac{1}{\lambda(k)}\left[P(k-1)-\frac{P(k-1)\varphi(k)\varphi^T(k)P(k-1)}{\lambda(k)+\varphi^T(k)P(k-1)\varphi(k)}\right] \tag{21c}$$

In this research, the identification algorithm is written as an S-Function in order to be used with the Real Time Windows Target Toolbox of Matlab. In order to get the solution quickly for on-line estimation, the Bierman UD factorization algorithm [17] is applied to compute the parameter estimation.

3.3 Derivation of predictor and calculation of control signal

The main idea of the predictive control algorithm is to compute the future control sequences that minimize the cost function Eq. (15). The future outputs are predicted using the linear difference equation Eq. (16). The parameters of the system model are obtained from the algorithm shown in section 3.2. The predictor and control signals can be derived in [15] as follows.

The difference equation Eq. (16) can be rewritten as a controlled autoregressive and integrated moving average (CARIMA) model as follows:

$$A(q^{-1})y(k)=B(q^{-1})u(k-1-d)+\frac{C(q^{-1})}{\Delta}\xi(k) \tag{22}$$

where:

$\zeta(k)$ is the process disturbance

$\Delta=1-q^{-1}$ is a different operator.

$A(q^{-1})=1+a_1q^{-1}+...+a_{na}q^{-na}$,

$B(q^{-1})=b_1+b_2q^{-1}+...+b_{nb}q^{-nb+1}$,

and $C(q^{-1})=1+c_1q^{-1}+...+c_{nb}q^{-nc}$ are polynomials in the backward shift operator q^{-1}.

na,nb,nc are the order of polynomials $A(q^{-1})$, $B(q^{-1})$, $C(q^{-1})$, respectively.

For simplicity, we assume that we consider the system without delay, so $d=0$. Then Eq. (22) can be rewritten as follows:

$$y(k)=\frac{B(q^{-1})}{A(q^{-1})}u(k-1)+\frac{C(q^{-1})}{A(q^{-1})\Delta}\xi(k) \tag{23}$$

At step j in the future, Eq. (23) becomes:

$$y(k+j)=\frac{B(q^{-1})}{A(q^{-1})}u(k+j-1)+\frac{C(q^{-1})}{A(q^{-1})\Delta}\xi(k+j) \tag{24}$$

$E_j(q^{-1}), F_j(q^{-1})$ are defined so that:

$$\frac{C(q^{-1})}{A(q^{-1})\Delta}=E_j(q^{-1})+q^{-j}\frac{F_j(q^{-1})}{A(q^{-1}).\Delta} \tag{25}$$

From Eq. (23), Eq. (24), and Eq. (25) we have:

$$\begin{aligned}y(k+j)=&\frac{E_j\left(q^{-1}\right)B\left(q^{-1}\right)}{C\left(q^{-1}\right)}\Delta u(k+j-1)+...\\&+\frac{F_j\left(q^{-1}\right)}{C\left(q^{-1}\right)}y(k)+E_j(q^{-1})\xi(k+j)\end{aligned} \tag{26}$$

Again, $G_j(q^{-1}), \Gamma_j(q^{-1})$ are defined to satisfy Eq. (27) as follows:

$$\frac{E_j(q^{-1})B(q^{-1})}{C(q^{-1})}=G_j(q^{-1})+q^{-j}\frac{\Gamma_j(q^{-1})}{C(q^{-1})} \tag{27}$$

Thus, the future output of the system is written:

$$\begin{aligned}y(k+j)=&G_j\left(q^{-1}\right)\Delta u(k+j-1)+\frac{\Gamma_j\left(q^{-1}\right)}{C\left(q^{-1}\right)}\Delta u(k-1)+...\\&+\frac{F_j\left(q^{-1}\right)}{C\left(q^{-1}\right)}y(k)+E_j\left(q^{-1}\right)\xi(k+j)\end{aligned} \tag{28}$$

The minimum variance prediction of $y(k+j)$ or given data up to time k is obtained by replacing the last term containing the future disturbance $\xi(k+j)$ by zeros, which yields:

$$\begin{aligned}\hat{y}(k+j)=&G_j(q^{-1})\Delta u(k+j-1)+...\\&+\frac{\Gamma_j(q^{-1})}{C(q^{-1})}\Delta u(k-1)+\frac{F_j(q^{-1})}{C(q^{-1})}y(k)\end{aligned} \tag{29}$$

Eq. (29) can be divided into two parts as follows:

$$y_0(k+j)=\frac{\Gamma_j(q^{-1})}{C(q^{-1})}\Delta u(k-1)+\frac{F_j(q^{-1})}{C(q^{-1})}y(k) \tag{30a}$$

which is called the *free response* of the system. That is the effect of the last control signal $u(k-1)$ on the future response.

Also,

$$\begin{aligned}\tilde{y}(k+j) &= G_j(q^{-1})\Delta u(k+j-1) \\ &= g_{j0}\Delta u(k+j-1)+... \\ &\quad + g_{j1}\Delta u(k+j-2)+...+g_{j,j-1}\Delta u(k)\end{aligned} \tag{30b}$$

which is the effect of future control signals on the future response.

$G_j(q^{-1})$ is the polynomial that contains the system step response coefficients. It can be defined from Eq. (25) and Eq. (27) as follows:

$$\frac{B}{\Delta A} = G_j + q^{-j}\Gamma_j + q^{-j}\frac{F_j B}{\Delta AC} \tag{31}$$

which shows that $G_j(q^{-1})$ is the quotient of the division $B/\Delta A$.

With the future outputs in Eq. (29), the control criterion Eq. (15) becomes:

$$J(u,t) = \sum_{j=1}^{N_2}\left[\hat{y}(k+j)-r(k+j)\right]^2 + \lambda\sum_{j=1}^{N_u}\left[\Delta u(k+j-1)\right]^2 \tag{32}$$

where

$$\begin{aligned}\hat{y}(k+j) = {} & g_0\Delta u(k+j-1)+g_1\Delta u(k+j-2)+... \\ & +...+g_{j-1}\Delta u(k)+y_0(k+j)\end{aligned}$$

In general, the above equation can be rewritten in the vector form as:

$$\hat{y} = G\Delta\tilde{u} + \tilde{y}_0 \tag{33}$$

where

$$G = \begin{bmatrix} g_0 & 0 & ... & 0 \\ g_1 & g_0 & ... & 0 \\ . & . & . & . \\ g_{N_u-1} & g_{N_u-2} & ... & g_0 \\ . & . & . & . \\ g_{N_2-1} & g_{N_2-2} & ... & g_{N_2-N_u} \end{bmatrix}$$

which is called the step coefficient matrix.

$$\begin{aligned}\tilde{y}_0 &= \left[y_0(k+1), y_0(k+2),..., y_0(k+N_2)\right]^T \\ \Delta\tilde{u} &= \left[\Delta u(k), \Delta u(k+1),..., \Delta u(k+N_u-1)\right]^T \\ \hat{y} &= \left[\hat{y}(k+1), \hat{y}(k+2),..., \hat{y}(k+N_2)\right]^T\end{aligned}$$

Then the cost function Eq. (32) becomes:

$$J = (\hat{y}-r)^T(\hat{y}-r) + \lambda\Delta\tilde{u}^T\Delta\tilde{u} \tag{34}$$

where $r = \left[r(k+1), r(k+2),..., r(k+N_2)\right]^T$ is a vector of desired signals in the future.

From Eq. (33) and Eq. (34) the cost function can be written as:

$$\begin{aligned}J &= (G\Delta\tilde{u}+\tilde{y}_0-r)^T(G\Delta\tilde{u}+\tilde{y}_0-r)+\lambda\Delta\tilde{u}^T\Delta\tilde{u} \\ &= \Delta\tilde{u}^T\left(G^TG+\lambda I\right)\Delta\tilde{u} + 2\left(\tilde{y}_0-r\right)^T G\Delta\tilde{u}\end{aligned}$$

To optimize the cost function J, the descend gradient method is used as follows:

$$gradient(J) = \frac{\partial J}{\partial\Delta\tilde{u}} = 0$$

From partial derivation, the following equation can be derived:

$$2\left(G^TG+\lambda I\right)\Delta\tilde{u} + 2\left(\tilde{y}_0-r\right)^T G = 0$$

From this equation, the control input can be obtained in Eq. (35):

$$\begin{aligned}\Delta\tilde{u} &= -\left(G^TG+\lambda I\right)^{-1}\left(\tilde{y}_0-r\right)^T G \\ &= \left(G^TG+\lambda I\right)^{-1}G^T\left(r-\tilde{y}_0\right)\end{aligned} \tag{35}$$

The control signal at time k is then computed as follows:

$$u(k) = u(k-1)+\Delta u(k) \tag{36}$$

Generally, with the time-delay system such as a slow response SMA system, the delay d-steps model in Eq. (16) is used:

$$A(q^{-1})y(k) = B(q^{-1})u(k-d-1) + \frac{C(q^{-1})}{\Delta}\xi(k)$$

Thus, Eq. (30) becomes:

$$\hat{y}(k+j) = G_j(q^{-1})\Delta u(k+j-d-1) + y_0(k+j) \tag{37}$$

Thus, Eq. (32) becomes:

$$J(u,t) = \sum_{j=N_1}^{N_2}\left[\hat{y}(t+j)-r(t+j)\right]^2 + \lambda\sum_{j=1}^{N_u}\left[\Delta u(t+j-1)\right]^2 \tag{38}$$

at $j = N_1$, $N_1 - d - 1 = 0$, so that $N_1 = d+1$.

Thus, only the $N = N_2 - N_1 + 1$ last rows of Eq. (30) are used. Then:

$$G=\begin{bmatrix} g_0 & 0 & ... & 0 \\ g_1 & g_0 & ... & 0 \\ . & . & . & . \\ g_{N_u-1} & g_{N_u-2} & \cdots & g_0 \\ . & . & . & . \\ g_{N-1} & g_{N-2} & \cdots & g_{N-N_u} \end{bmatrix}, \text{ with } N=N_2-N_1+1 \tag{39}$$

and

$$\tilde{y}_0=\left[y_0(k+N_1), y_0(k+N_1+1),..., y_0(k+N_2)\right]^T$$

3.4 The solution of the step coefficient matrix and free response:

The control signals in Eq. (35) can be obtained easily if G and $\tilde{y}_0$ are computed. One way to obtain G and $\tilde{y}_0$ is to solve the Diaphantine functions Eq. (25) and Eq. (27) to get E_j, F_j, G_j and Γ_j; then G and y_0 can be obtained using Eq. (34) and Eq. (30a). However, this way is very complicated and time consuming. In this paper, a simple and useful way to obtain G and $\tilde{y}_0$ is derived. In this way, G and $\tilde{y}_0$ are obtained directly from the system model as follows:

Eq. (23) can be written:

$$\Delta A y(k)=B(q^{-1})\Delta u(k)+C(q^{-1})\xi(k)$$
$$\text{or } (1-q^{-1})Ay(k)=B(q^{-1})\Delta u(k)+C(q^{-1})\xi(k)$$

Then, the output at sampling time k can be obtained:

$$y(k)=y(k-1)-\left(1-q^{-1}\right)(A-1)y(k)+... \\ +B(q^{-1})\Delta u(k)+C(q^{-1})\xi(k)$$

or

$$y(k)=My(k)+B(q^{-1})\Delta u(k)+C(q^{-1})\xi(k) \tag{40}$$

where

$$\begin{aligned} &B=b_1q^{-1}+b_2q^{-2}+...+b_{nb}q^{-nb} \\ &M=m_1q^{-1}+m_2q^{-2}+...+m_{nm}q^{-nm},\ \ nm=na+1 \\ &m_1=1-\mathrm{a}_1 \\ &m_2=\mathrm{a}_1\text{-}\mathrm{a}_2 \\ &... \\ &m_i=a_{i-1}-a_i \\ &... \\ &m_{nm}=a_{na} \end{aligned} \tag{41}$$

In the other way, Eq. (31) can be written in the form of a series as follows:

$$y(k)=\sum_{i=1}^{nm}m_iy(k-i)+\sum_{i=1}^{nb}b_i\Delta u(k-i)+\sum_{i=1}^{nc}c_i\xi(k-i)$$

Choose: $C(q^{-1})=1$. Then,

$$y(k)=\sum_{i=1}^{nm}m_iy(k-i)+\sum_{i=1}^{nb}b_i\Delta u(k-i)+\xi(k)$$

Then, at the future time $k+j$:

$$y(k+j)=\sum_{i=1}^{nm}m_iy(k-i+j)+\sum_{i=1}^{nb}b_i\Delta u(k-i+j)+\xi(k+j)$$

The control objective is $\xi(k+j)=0$, thus, (35) becomes:

$$y(k+j)=\sum_{i=1}^{nm}m_iy(k-i+j)+\sum_{i=1}^{nb}b_i\Delta u(k-i+j)$$

or

$$y(k+j)=y_j=y_{ju}+y_{j0}$$

where y_{j0} is defined as a *free response*, which depends only on past signals, so that:

$$\begin{aligned} y_{10}&=\sum_{i=1}^{nm}m_iy(k-i+1)+\sum_{i=2}^{nb}b_i\Delta u(k-i+1) \\ y_{20}&=m_1y_{10}+\sum_{i=2}^{nm}m_iy(k-i+2)+\sum_{i=3}^{nb}b_i\Delta u(k-i+2) \\ &... \\ y_{j0}&=\sum_{i=1}^{\min(j-1,nm)}m_iy_{(j-i)0}+\sum_{i=j}^{nm}m_iy(k-i+j)+... \\ &\quad+\sum_{i=j+1}^{nb}b_i\Delta u(k-i+j) \end{aligned} \tag{42}$$

and y_{ju} is the term that depends on the future control signals. Thus,

$$\begin{aligned} y_{1u}&=b_1\Delta u(k)=g_0\Delta u(k) \\ y_{2u}&=m_1y_{1u}+b_1\Delta u(k+1)+b_2\Delta u(k) \\ &=b_1\Delta u(k+1)+\left(m_1g_1+b_2\right)\Delta u(k) \\ &=g_1\Delta u(k+1)+g_2\Delta u(k) \\ y_{3u}&=m_1y_{2u}+m_2y_{1u}+\sum_{i=1}^{3}b_i\Delta u(k+3-i) \\ &=b_1\Delta u(k+2)+\left(m_1g_1+b_2\right)\Delta u(k+1)+... \\ &\quad+\left(m_1g_2+m_2g_1+b_3\right)\Delta u(k) \\ &=\sum_{i=1}^{3}g_i\Delta u(k+3-i) \end{aligned}$$

In summary,

$$\begin{aligned} y_{ju}&=\sum_{i=1}^{\min(j-1,na)}m_iy_{(j-i)u}+\sum_{i=1}^{\min(j,nb)}b_i\Delta u(k+j-i) \\ &=\sum_{i=1}^{j}g_i\Delta u(k+j-i) \\ g_j&=\begin{cases}\sum_{i=1}^{\min(j,na)}g_im_{j-i}+b_j, & j\le nb \\ \sum_{i=1}^{\min(j,na)}g_im_{j-i}, & j>nb\end{cases} \end{aligned} \tag{43}$$

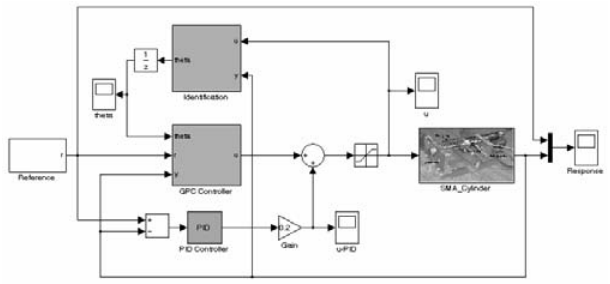

Fig. 10. Matlab schematic diagram of the predictive controller applied to SMA cylinder.

In summary, the predictive control algorithm used in this research is implemented through the following steps:

(1) Compute parameters for the model Eq. (16) using Eq. (21);

(2) Determine the system step response coefficients matrix using Eq. (43);

(3) Determine the free response $y_0(t+j)$ using Eq. (42);

(4) Find the increment control signals vector $\Delta\tilde{u}$ from Eq. (35);

(5) Find the control signal vector $u(k)$ from Eq. (36);

(6) Repeat the first step.

In this research, the program-implemented predictive algorithm is also written as an S-Function block in order to be used with the Real Time Windows Target Toolbox of Matlab.

4. Position and force control of SMA cylinder

This section presents the experimental results of the real time position and force control of the proposed SMA cylinder by using the predictive control and conventional PID algorithm. The experiments were implemented at room temperature (25^0C). Sampling time was set to 0.01 s in all experiments.

The generalized predictive control scheme applied to the SMA cylinder control system is shown in Fig. 10. There are three inputs to the controller: *theta* is the estimated parameters of the system model, r is the reference position or force, and y is the real value of the position or force measured by the SMA cylinder. The input current applied to the SMA cylinder is obtained from the predictive algorithm.

The PID controller is added into the GPC controller to generate the control signal for online identification at the beginning.

4.1 Position control results

The position control results are shown in Figs. 11, 15, 16, 17, and 19. The predictive control parameters are selected as follows:

$$N_1 = 5,\ N_2 = 15,\ N_u = 6,\ n_a = 5,\ n_b = 4, \lambda = 0.01 .$$

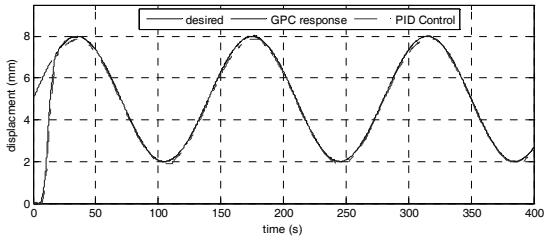

(a) System response

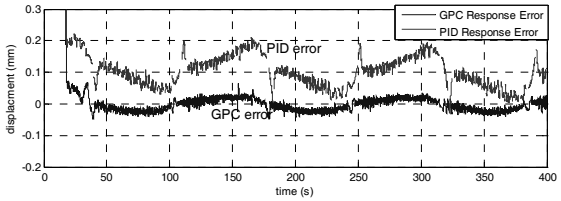

(b) Control error

Fig. 11. System response and control error of cylinder with respect to sinusoidal input.

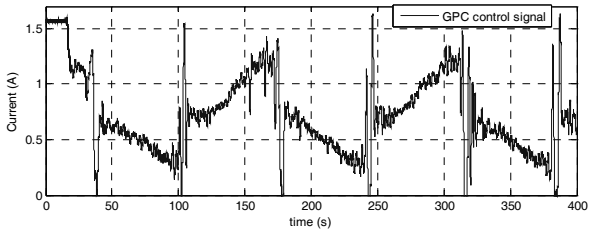

(a) Control signal of GPC.

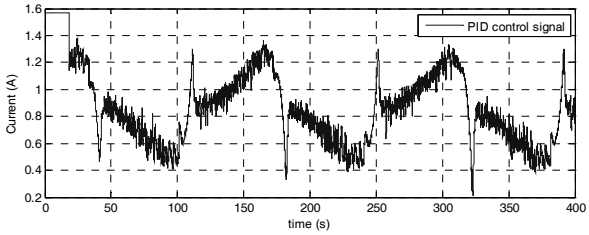

(b) Control signal of PID Controller

Fig. 12. Control input current for sinusoidal response.

Initial values of online identification are chosen:

$$\theta_0 = 0, P = 10^{10} eye(9), \lambda = 0.99$$

The PID parameters used in this case are chosen by trial and error:

$$K_p = 9,\ K_i = 0.07,\ K_d = 0.2 .$$

Fig. 11 shows the system responses with respect to sinusoidal input. It can be seen that the system has a very slow response and greater overshoot when the conventional PID controller is used.

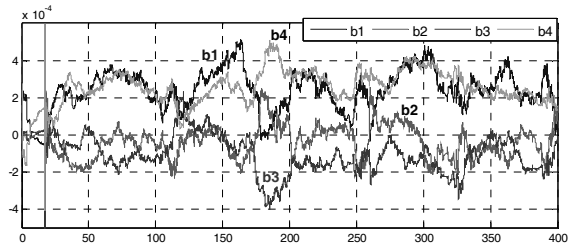

(a) Numerator parameters

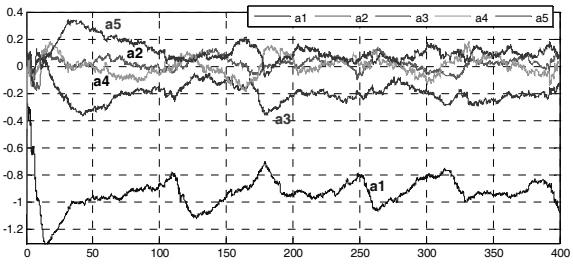

(b) Denominator parameters

Fig. 13. Position model parameter estimation.

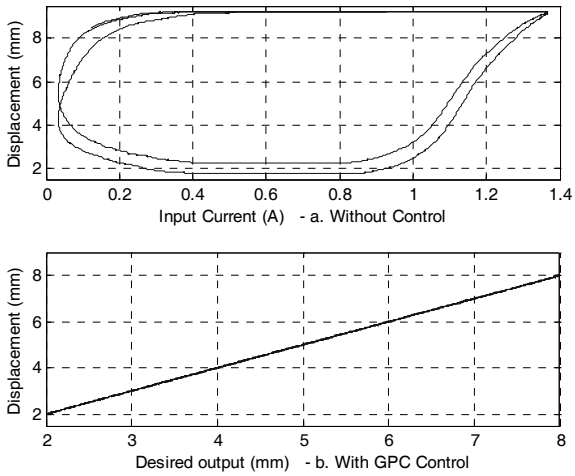

Fig. 14. Hysteresis characteristics of SMA cylinder before and after applying GPC.

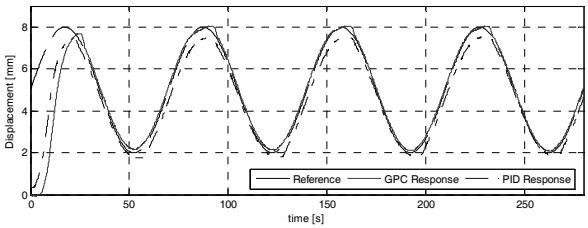

Fig. 15. Sinusoidal response at frequency 1/70 Hz.

Figs. 14(a) and 14(b) show hysteresis curves of the sinusoidal response in Fig. 11 before and after applying the GPC controller, respectively. The hysteresis phenomenon is almost completely offset.

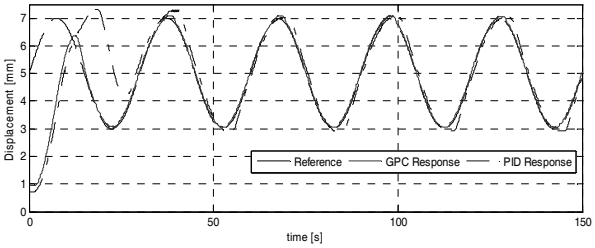

Fig. 16. Sinusoidal response at frequency 1/30 Hz.

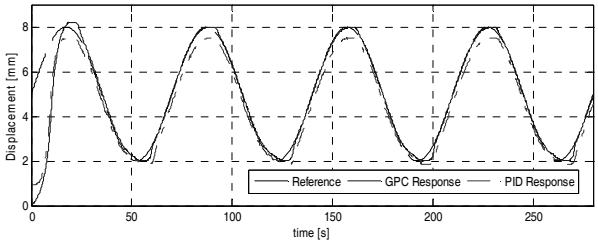

Fig. 17. Sinusoidal response at frequency 1/70 Hz with external load *F=2N*.

GPC is also applied to control the cylinder position for different conditions of frequency (Fig. 15 and 16) and load (Fig. 17). The results show that the GPC can be tracked well with the reference.

4.2 Force control results

Step responses with respect to different reference forces (at the position of 4 mm) of the conventional PID and predictive controllers are shown in Fig. 17.

The predictive control parameters are selected as follows:

$$N_1 = 5,\ N_2 = 20,\ N_u = 7,\ n_a = 5,\ n_b = 4, \lambda = 0.01$$

The initial value of online identification is:

$$\theta_0 = 0,\ P = 10^7 eye(9),\ \lambda = 0.97$$

The PID parameters used in this case are chosen by trial and error:

$$K_p = 8,\ K_i = 0.1,\ K_d = 0.08\ .$$

These experimental results demonstrate that the predictive controller can be used to improve the force control performance of the proposed SMA cylinder.

Although the force generated from the SMA cylinder was small, the predictive controller could achieve better responses than those of the conventional PID controller, especially with tracking control.

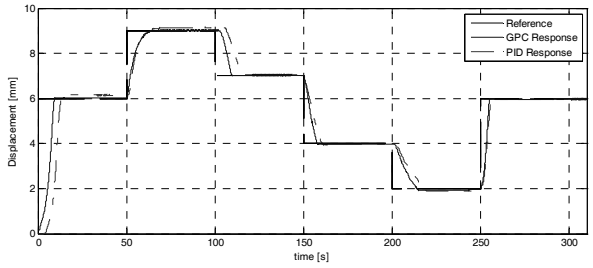

Fig. 18. Step reponse of position control of SMA cylinder.

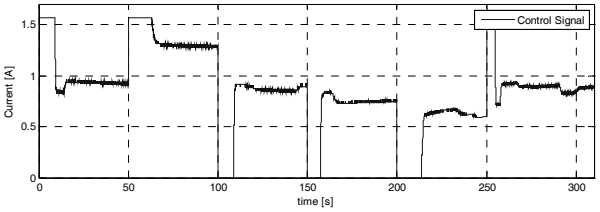

Fig. 19. GPC Control input.

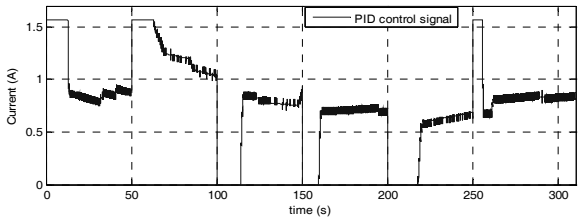

Fig. 20. PID Control input.

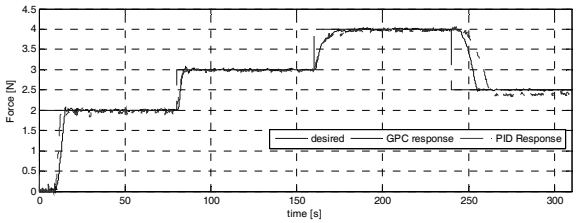

Fig. 21. Step reponse of force control of SMA cylinder.

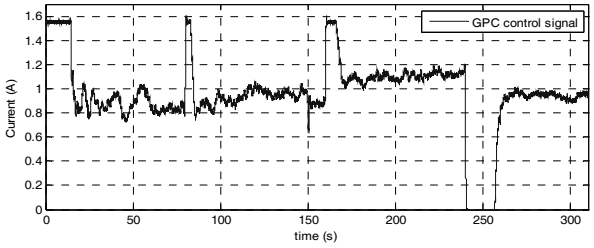

Fig. 22. GPC Control input.

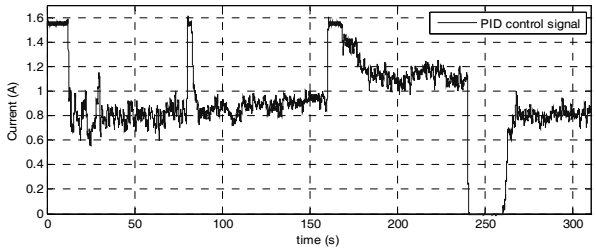

Fig. 23. PID Control input.

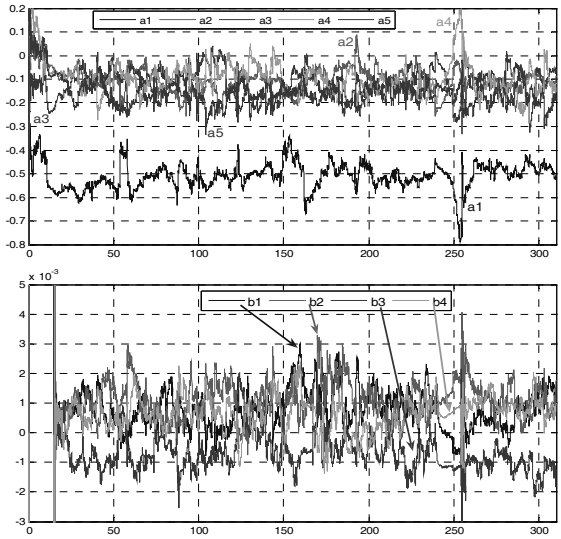

Fig. 24. Model tuning parameters.

5. Conclusions

In this work, we fabricated a linear motion actuator that functions like an electric cylinder using a SMA spring. The GPC was investigated as a method to offset the SMA hysteresis phenomenon. The control algorithm based on the predicted output behavior of the SMA actuator was successfully applied to control the position and force of the proposed SMA cylinder. Experimental results showed that the applied control method can be used to improve the control performance, and therefore reduce the hysteresis nonlinearity of the SMA actuators. The proposed controller was also compared to the conventional PID controller, and was shown to perform better than a conventional controller. This control method is effective not only for SMA actuators, but also for other actuators with hysteresis.

Acknowledgements

This work was supported by the BK21, Korea Research Foundation.

References

[1] Z. W. Zhong and C. K. Yeong, Development of a gripper using SMA wire, *Sensors and Actuators A: Physical*, 126 (2)

(2006) 375-381.
[2] G. Shuxiang, O. Junsei and F. Toshio, A Novel Type of Micropump Using SMA Actuator for Microflow Application, *IEEE International Conference on Robotics and Automation* (2003) 987-992.
[3] J. J. R. V. Patel and S. N. M. Ostojic, Modelling and Gain Scheduled Control of Shape Memory Alloy Actuators, *Proc. of the 2005 IEEE Conf. on Control Applications*, Toronto, Canada; (2005) 767-772.
[4] M. H. Elahinia and H. Ashrafiuon, Nonlinear Control of a Shape Memory Alloy Actuated Manipulator, *Trans. of the ASME*, 124 (2002) 566-575.
[5] K. K. Ahn and N. B. Kha, Improvement of the performance of hysteresis compensation in SMA actuators by using inverse Preisach model in closed – loop control system, *Journal of Mechanical Science and Technology*, 20 (5) (2006) 634-642.
[6] K. K. Ahn and N. B. Kha, Internal model control for shape memory alloy actuators using fuzzy based Preisach model, *Sensors and Actuators A: Physical*, 136 (2) (2007) 730-741.
[7] G. Song, V. Chaudhry and C. Batur, Precision tracking control of shape memory alloy actuators using neural networks and a sliding-mode based robust controller, *Smart Materials And Structures* (2003) 223-231.
[8] D. W. Clarke, C. Mohtadi and P. S. Tuffs, 1987, Generalized predictive control – Part 1. The Basic Algorithm, *Automatica,* 23 (2) 137-148.
[9] D. W. Clarke, Application of generalized predictive control to industrial processes, *IEEE Control Systems Magazine* (1988) 49-55.
[10] J. B. Rawlings, Tutorial overview of model predictive control, *IEEE Control Systems Magazine* (2000) 38-52.
[11] F. Allgower and A. Zheng, *Nonlinear Model Predictive Control*, Birkhauser Verlag, Germany (2000).
[12] B. Kouvaritakis, M. Cannon, *Nonlinear Predictive Control – Theory and Practice*, IEE, London (2001).
[13] T. Waram, Design principles for Ni-Ti actuators, *Engineering aspects of shape memory alloys*, Butterworth-Heinemann (1990) 234-244.
[14] D. Dumur and P. Boucher, A Review Introduction to Linear GPC and Applications, *Journal A*, 39 (4) (1998) 21-35.
[15] J. Mikleš and M. Fikar, *Process Modelling, Identification, and Control*, Springer (2007).
[16] L. Ljung, *System Identification*, Prentice Hall (1999).
[17] G. J. Bierman, Factorization Methods for Discrete Sequential Estimations, *Academic Press*, New York (1997).

Nguyen Trong Tai received the B.S. and M.S. degrees from Hochiminh City University of Technology in 2005 and 2008, respectively, all in Automatic Control Engineering. He is currently studying Ph.D. Course at University of Ulsan. His research interests focus on intelligent control, modern control theory and their applications, design and control of smart actuator systems.

Kyoung Kwan Ahn received a B.S. degree in Mechanical Engineering from Seoul National University in 1990, an M. Sc. degree in Mechanical Engineering from the Korea Advanced Institute of Science and Technology (KAIST) in 1992, and a Ph.D. degree (dissertation title: "A study on the automation of outdoor tasks using 2 link electro-hydraulic manipulator") from the Tokyo Institute of Technology in 1999, respectively. He is currently a Professor in the School of Mechanical and Automotive Engineering, University of Ulsan, Ulsan, Korea. His research interests are design and control of smart actuator using smart material, fluid power control and active damping control. He is a Member of IEEE, ASME, SICE, RSJ, JSME, KSME, KSPE, KSAE, KFPS, and JFPS.